Carbohydrate Polymers 89 (2012) 802–809

Contents lists available at SciVerse ScienceDirect

Carbohydrate Polymers

journal homepage: www.elsevier.com/locate/carbpol

Quantification of crystalline cellulose in lignocellulosic biomass using sum frequency generation (SFG) vibration spectroscopy and comparison with other analytical methods

Anna L. Barnette[a], Christopher Lee[a], Laura C. Bradley[a], Edward P. Schreiner[a], Yong Bum Park[b], Heenae Shin[c,d], Daniel J. Cosgrove[b], Sunkyu Park[c,d,*], Seong H. Kim[a,e,**]

[a] Department of Chemical Engineering, Pennsylvania State University, University Park, PA 16802, United States
[b] Department of Biology, Pennsylvania State University, University Park, PA 16802, United States
[c] Department of Forest Biomaterials, North Carolina State University, Raleigh, NC 27695, United States
[d] Department of Forest Sciences, Seoul National University, Seoul, Republic of Korea
[e] Materials Research Institute, Pennsylvania State University, University Park, PA 16802, United States

ARTICLE INFO

Article history:
Received 11 November 2011
Received in revised form 4 April 2012
Accepted 5 April 2012
Available online 20 April 2012

Keywords:
Cellulose
Crystallinity
Sum frequency generation
X-ray diffraction
FT-Raman

ABSTRACT

The non-centrosymmetry requirement of sum frequency generation (SFG) vibration spectroscopy allows the detection and quantification of crystalline cellulose in lignocellulose biomass without spectral interferences from hemicelluloses and lignin. This paper shows a correlation between the amount of crystalline cellulose in biomass and the SFG signal intensity. Model biomass samples were prepared by mixing commercially available cellulose, xylan, and lignin to defined concentrations. The SFG signal intensity was found sensitive to a wide range of crystallinity, but varied non-linearly with the mass fraction of cellulose in the samples. This might be due to the matrix effects such as light scattering and absorption by xylan and lignin, as well as the non-linear density dependence of the SFG process itself. Comparison with other techniques such as XRD, FT-Raman, FT-IR and NMR demonstrate that SFG can be a complementary and sensitive tool to assess crystalline cellulose in biomass.

1. Introduction

Cellulose is the most abundant biopolymer on earth (Jarvis, 2003; Kim, Yun & Ounaies, 2006; Wada, Ike & Tokuyasu, 2010). Beyond its traditional use as raw materials for papers and textiles, it also has applications in microdevices (Kim et al., 2006; Zhao & Berg, 2008), coatings (Kim et al., 2006), composite materials (Pérez & Samain, 2010), and renewable fuels (Park, Johnson, Ishazawa, Parilla & Davis, 2009). The crystalline structure of cellulose can provide mechanical rigidity and toughness for composite materials. It is a source of recalcitrance of lignocellulosic biomass against deconstructive processes (Zhang & Lynd, 2004). Also, crystalline cellulose influences wall extensibility, which is a key determinant of plant growth and differentiation (Schindelman et al., 2001). In all these cases, it is critically important to find the nature and amount of crystalline cellulose in a given sample to understand the structural roles of cellulose in the biological, mechanical, and recalcitrant properties of plant cell walls. Many studies have been performed for several decades to quantify the crystalline cellulose in intact lignocellulosic biomass for better understanding and usage of cellulose (Amim, Kosaka, Petri, Maia & Miranda, 2009; Cael, Gardner, Koenig & Blackwell, 1975; Hall, Bansal, Lee, Realff & Bommarius, 2010; Katoaka & Kondo, 1998; Kondo, 1997; Kovalenko, 2010; Langan, Sukumar, Nishiyama & Chanzy, 2005; Marrinan & Mann, 1954; Park, Baker, Himmel, Parilla & Johnson, 2010; Wada, Chanzy, Nishiyama & Langan, 2004).

The terminology 'crystallinity' is defined as the fraction of crystalline cellulose in the sample analyzed. When the test sample is purified cellulose, then the calculated crystallinity is the fraction of crystalline phase over the total amount of cellulose, which is called 'cellulose crystallinity' (Park et al., 2010). When the test sample is lignocellulose biomass, the calculated value is the fraction of crystalline cellulose in the entire sample including hemicellulose and lignin. This could be called 'sample crystallinity'. Though these definitions are obviously different, these two terms were often used in the literature without clear distinction. The crystallinity can be calculated from X-ray diffraction (XRD) (Langan et al., 2005; Park et al., 2010; Wada et al., 2004) or other spectroscopic methods

* Corresponding author at: Department of Forest Biomaterials, North Carolina State University, Raleigh, NC 27695, United States.
** Corresponding author at: Department of Chemical Engineering, Pennsylvania State University, University Park, PA 16802, United States.
E-mail addresses: sunkyu_park@ncsu.edu (S. Park), shkim@engr.psu.edu (S.H. Kim).

0144-8617/$ – see front matter © 2012 Elsevier Ltd. All rights reserved.
http://dx.doi.org/10.1016/j.carbpol.2012.04.014

such as solid-state ^{13}C nuclear magnetic resonance (NMR), Raman spectroscopy (Agarwal, Reiner & Ralph, 2010; Schenzel, Fischer & Brendler, 2005), and Fourier transform infrared spectroscopy (FT-IR) (Kono, Erata & Takai, 2002; Kono et al., 2002b; Park et al., 2009).

Typical powder XRD of plant cell walls such as woods shows diffraction peaks centered at ~14.9°, ~16.7°, ~22.9°, and ~34.5°. These correspond to diffraction peaks of the $(\bar{1}\,1\,0)$, $(1\,1\,0)$, $(2\,0\,0)$, and $(0\,0\,4)$ crystallographic planes, respectively, of cellulose Iβ which is the main allomorph of cellulose produced by vascular plants (Driemeier & Calligaris, 2011). In the Meyer–Misch model commonly cited in cellulose literature, these peaks correspond to $(1\,0\,1)$, $(1\,0\,\bar{1})$, $(0\,0\,2)$, and $(0\,4\,0)$, respectively (Meyer & Misch, 1937). Hemicellulose, lignin, and amorphous cellulose give a diffuse scattering halo between 12 and 27° (Hatakeyama & Hatakeyama, 1982; Isogai, 1994; Park et al., 2010; Thygesen, Oddershede, Lilholt, Thomsen & Stahl, 2005). The width of the crystalline diffraction peak can be used to estimate the average size of cellulose crystallites (Hindeleh & Johnson, 1972, 1974). The relative intensity ratio of the diffraction peak and the amorphous halo intensity can be used to calculate the sample crystallinity, i.e. the amount of crystalline cellulose in lignocellulosic biomass (Park et al., 2010; Segal, Creely, Martin & Conrad, 1959; Thygesen et al., 2005). To estimate the crystalline cellulose fraction in the sample from powder XRD, a few methods have been developed (Park et al., 2010). The 'peak height' method developed by Segal and coworkers is the most widely used due to its simplicity (Segal et al., 1959). In this method, the crystallinity is calculated as the ratio of the height of the 2 0 0 peak (I_{200} at ~22.9°) and the height of the amorphous scattering minimum (I_{AM} at ~18.3°). This method is useful for comparing the relative differences between samples; however it has been reported that the calculated value from the peak height method overestimates the true crystalline portion (Park et al., 2010).

In ^{13}C NMR, each carbon atom in the glucopyranose unit exhibits different chemical shift due to subtle difference in magnetic field shielding by neighboring atoms (Isogai, 1994; Isogai, Usuda, Kato, Uryu & Atalla, 1989; Wan, wang & Xiao, 2010). The chemical shifts of the C4 and C6 carbons are especially sensitive to the cellulose structure. The crystalline structure of cellulose generates sharp peaks at higher chemical shifts (~89 ppm for C4 and ~66 ppm for C6) while the amorphous structure gives broad peaks at slightly lower chemical shifts (~84 ppm for C4 and ~63 ppm for C6) (Isogai, 1994; Isogai et al., 1989; Wan et al., 2010). The ratio of these two peaks in ^{13}C NMR can be used to calculate the crystallinity of cellulose (Whitney, Brigham, Darke, Grant Reid, & Gidley, 1995). The analysis for lignocellulosic biomass needs caution since cellulose peaks overlap with peaks from hemicellulose and lignin.

Fourier transform Raman spectroscopy (FT-Raman) has been employed to quantify sample crystallinity. The CH_2 bending vibration of exocyclic group in the crystalline and amorphous cellulose appears as 1481 cm^{-1} and 1462 cm^{-1}, respectively. Thus, the ratio of these two peaks could be used for crystallinity calculations (Schenzel et al., 2005). Agarwal et al. (2010) reported that it would be easier and more accurate to use the intensity of the 380 cm^{-1} peak originating from skeletal bending of the crystalline phase normalized with the intensity of the 1096 cm^{-1} peak attributed to CC or CO stretching (Wiley & Atalla, 1987).

Fourier transform infrared spectroscopy (FTIR) has also been used since it is readily available in many laboratories (Cael et al., 1975; Katoaka & Kondo, 1998; Kondo, 1997; Kondo & Sawatari, 1996; Marrinan & Mann, 1954) and certain vibration peaks in the finger print region (700–1500 cm^{-1}) are sensitive to cellulose crystalline structure (Oh et al., 2005). However, crystallinity analysis with FT-IR is cumbersome because multicomponent solids often give broad features which can overlap and conceal crystalline peaks, necessitating deconvolution (Atalla, 1999; Cael et al., 1975; Marrinan & Mann, 1954). Deconvolution of crystalline peaks is sensitive to background subtraction, and a calibration standard developed from XRD or solid-state ^{13}C NMR is necessary (Meier, 2005).

The interference or baseline correction problems due to amorphous components in the sample can be avoided if one uses a technique that specifically detects the crystalline cellulose and is intrinsically insensitive to amorphous phases. It has been demonstrated that sum frequency generation (SFG) vibration spectroscopy meets these requirements (Barnette et al., 2011). SFG is a second-order nonlinear optical response of materials lacking centrosymmetry (Held, Lvovsky, Wei & Shen, 2002; Lambert, Davies & Neivandt, 2005; Miranda & Shen, 1999; Shen, 1989). The frequency of the SFG signal emitted is the sum of the visible and IR frequencies of the irradiated laser pulses: $\omega_{SFG} = \omega_{VIS} + \omega_{IR}$. The SFG signal intensity $I(\omega_{SFG})$ is given in Eq. (1) (Vidal & Tadjeddine, 2005):

$$I(\omega_{SFG}) \propto \left|\chi^{(2)}_{eff}\right|^2 I(\omega_{VIS}) I(\omega_{IR}) \tag{1}$$

where $I(\omega_{VIS})$ and $I(\omega_{IR})$ are the intensities of the visible and infrared incident beams, respectively, and $\chi^{(2)}_{eff}$ is the effective nonlinear susceptibility, which can be expressed as (Held et al., 2002; Lambert et al., 2005; Miranda & Shen, 1999; Shen, 1989):

$$\chi^{(2)}_{eff} = \frac{N \sum_{\alpha,\beta,\gamma} \langle M_{\alpha\beta} A_{\gamma} \rangle}{\varepsilon_o (\omega_{IR} - \omega_q - i\Gamma)} \tag{2}$$

where N is the number density of specific vibration modes, $\langle M_{\alpha\beta} A_{\gamma} \rangle$ is the angle-average of the product of the Raman and infrared tensors of a normal vibration mode, ε_o is the dielectric constant of vacuum, ω_q is the frequency of the normal vibration mode, and Γ is the damping constant. Non-zero $\chi^{(2)}_{eff}$ value exists only when the vibration mode is both Raman- and IR-active and arranged non-centrosymmetrically in optical space.

With these unique features, the selective detection of crystalline cellulose in biomass was demonstrated with SFG vibration spectroscopy in a qualitative manner and no peak was identified with other cell wall components such as hemicellulose and lignin (Barnette et al., 2011). In this paper, the correlation was investigated between the SFG signal intensity and the crystalline cellulose concentration in lignocellulosic biomass, which could lead to development of a new method calculating the sample crystallinity. Model biomass samples with known cellulose amounts were prepared, for simplicity, by mixing commercially available microcrystalline cellulose, xylan, and lignin; these model samples were then analyzed with SFG, XRD, NMR, FT-Raman, and FT-IR. The SFG signal intensity was found to vary non-linearly with the crystalline cellulose content in the model biomass samples. With a proper calibration curve, SFG can be used to estimate the amount of the crystalline cellulose in wood cell walls without any chemical treatments. The absence of peaks from hemicellulose and lignin makes SFG analysis highly attractive for direct analysis of crystalline cellulose in lignocellulosic biomass. However, there are several parameters limiting the accuracy of the SFG-based crystallinity estimation.

2. Experimental methods

2.1. Sample preparation

Avicel® PH-101 (microcrystalline cellulose, CAS-No. 9004-34-6) consisting of mostly cellulose I_β, xylan (from beech wood, CAS-No. 9014-63-5), and lignin (alkali lignin, CAS-No. 8068-05-1) were purchased from Sigma-Aldrich and used as received. The structure and composition of cellulose, hemicellulose, and lignin in biomass vary

depending on the source (plants) and chemical treatments during the sample preparation. In this study, we used the commercially available and most-commonly-used samples as a model biomass. In order to investigate the effect of the amount of cellulose on the measurements, powder mixtures of cellulose, xylan, lignin were prepared with varying mass fractions of cellulose from zero to one while keeping the xylan:lignin ratio constant at 1:1. This relative ratio of xylan and lignin was chosen to mimic typical composition of wood samples. All mixtures were pressed into pellets at 650 bar and used for SFG, XRD, FT-Raman, and FT-IR analyses. NMR analysis was carried out for pure components only. Small wood chips of Scandinavian pine (*Pinus sylvestris*) and Scarlet oak (*Quercus coccinea*) were used for SFG analysis without any modifications. The chemical compositions of wood samples were analyzed by ethanol/benzene extraction and Klason lignin procedure followed by high performance liquid chromatography (HPLC) sugar analysis (Sluiter et al., 2008).

2.2. Sum frequency generation (SFG) vibration spectroscopy measurements

All physical mixtures and pure samples were analyzed using a SFG spectrometer (EKSPLA) pumped by a picosecond Nd:YAG laser, 1064 nm at 10 Hz. The 1064 nm pulse was frequency doubled to 532 nm in the visible range, and the (OPG/OPA) functions to tune the 2.3–10 μm infrared region using an $AgGaS_2$ crystal. An IR (p-polarized) beam at 56° from the surface normal and a visible (s-polarized) beam at 60° were overlapped spatially and temporally on each sample and the SFG signal was measured at a reflection geometry (Barnette et al., 2011). The scattered SFG signal was collected using a beam collimator filtered with as polarizer and a monochromator, and detected with a photomultiplier tube (Hamamatsu Corp.). SFG spectra were taken at 4 cm^{-1} steps in the CH region (2700–3000 cm^{-1}) and 8 cm^{-1} steps in the OH region (3000–3800 cm^{-1}) and. Each step was an average of 100 pulses. The measured SFG intensity was divided with IR and visible input laser intensities, $I_{SFG}/(I_{VIS} \times I_{IR})$, to compensate the variation of the excitation light intensities. SFG spectra of wood samples were taken for the early wood region in ambient air with the laser incidence plane parallel to the growth direction.

2.3. X-ray diffraction (XRD) measurements

XRD experiments were performed using a Rigaku SmartLab X-ray diffraction with a Cu tube (λ = 1.5405 Å). The radiation was generated at 25 mA and 35 kV. The scattering angle of 2θ from 9° to 41° was measured at the step size of 0.05° with 5 s exposure at each step. Three methods such as peak height, peak deconvolution, and amorphous subtraction methods were compared to evaluate the cellulose crystallinity of samples from XRD patterns (Park et al., 2010, 2009). In the peak height method, the crystallinity was calculated from the intensity ratio between the crystalline peak at ~22.9° and the amorphous background at ~18.3°. In the peak deconvolution method, a peak fitting program (PeakFit, www.systat.com) was used to extract individual crystalline peaks from the diffraction intensity profiles, assuming Gaussian functions for each peak and a broad halo at ~21.5° as amorphous contribution. In the amorphous subtraction method, the XRD data of the xylan and lignin powder mixture was used as an amorphous standard to subtract the amorphous portion from the diffraction profiles. A scale factor was applied to the amorphous standard spectrum, so that the baseline between the crystalline XRD peaks is zero without any negative values after subtraction of the amorphous portion. The detailed procedures were described elsewhere (Park et al., 2010).

2.4. Fourier transform Raman (FT-Raman) measurements

Mixture and pure pellets were analyzed with a Nicolet 8700 FT-Raman spectrometer (Thermo Scientific). The excitation source was a diode-pumped Nd:YAG laser (1064 nm); the signal was collected with a liquid nitrogen cooled germanium detector. The Fourier transform spectra were analyzed in a region 250–3750 cm^{-1} with an 8 cm^{-1} step. All spectra were the average of 1000 scans. To eliminate sample burning during a scan, the excitation beam power was decreased to 0.1–1 mW and defocused. Each spectrum shown here was an average of triplicate measurements.

2.5. Fourier transform infrared (FT-IR) measurements

FTIR spectra of physical mixture and pure samples were measured using a Thermo Nicolet Nexus 760 FT-IR spectrometer (Thermo Scientific), equipped with a deuterated triglycine sulfate (DTGS) detector. Each spectrum was an average of 100 scans from 500 cm^{-1} to 4000 cm^{-1}, at a resolution of 2 cm^{-1}. In addition to sample preparation described earlier, pellets were mixed with a mass fraction of 5–6% KBr (Sigma–Aldrich) and pressed at 650 bar, for attenuation of IR absorption.

2.6. Solid state ^{13}C nuclear magnetic resonance (NMR) measurements

High-resolution solid-state ^{13}C NMR spectra were collected at 9.4 T with cross-polarization and magic angle spinning (CP/MAS) in a Bruker Avance 400 MHz spectrometer. ^{1}H and ^{13}C fields were matched at 53.6 kHz and a 1 dB ramp was applied to the proton rotating-frame during the matching period. Acquisition time was 0.034 s and sweep-width was 30 kHz. Magic-angle spinning was performed at 7000 Hz. 3000 scans were averaged using a 2 ms contact time and a delay time of 4.0 s. CP/MAS experiment is not quantitative due to differences in cross polarization rates and rotating frame relaxation times; however, differences observed in relative peak intensities and integrated areas can be used to identify differences between similar samples.

3. Results and discussion

3.1. Characterization of model biomass mixture

3.1.1. SFG analysis

The main focus of this study was to evaluate the capability of SFG to prove changes in the amount of crystalline cellulose in lignocellulosic biomass or 'sample crystallinity'. For that reason, the model biomass samples were prepared with a commonly available cellulose, hemicellulose and lignin. Fig. 1a displays SFG spectra of model biomass samples (Avicel, xylan, and lignin) and their mixtures. The non-cellulosic components (xylan and lignin) show no peak, while cellulose shows unique features in SFG spectra. The details of peak assignment were published previously (Barnette et al., 2011). In brief, the peak at 2945 cm^{-1} is attributed to the asymmetric vibration of the CH_2 group at the exocyclic side chain of cellulose I_β. The weak peak at 2850 cm^{-1} can be attributed to symmetric stretching vibrations of the CH_2 group. The axial C–H groups in the glucopyranose ring of cellulose I_β are usually detected at 2902 cm^{-1} in IR and 2898 cm^{-1} in Raman; but they are not detected in SFG due to symmetry cancellation in the crystalline cellulose structure. The 3325 cm^{-1} peak in SFG is tentatively assigned to the ^{3}O–H hydrogen-bonded to ^{5}O and ^{2}O–H hydrogen-bonded to ^{6}O which have the transition dipole close to the chain axis direction. Other O–H peaks of cellulose I_β and all O–H peaks in hemicellulose and lignin are not detected in SFG because

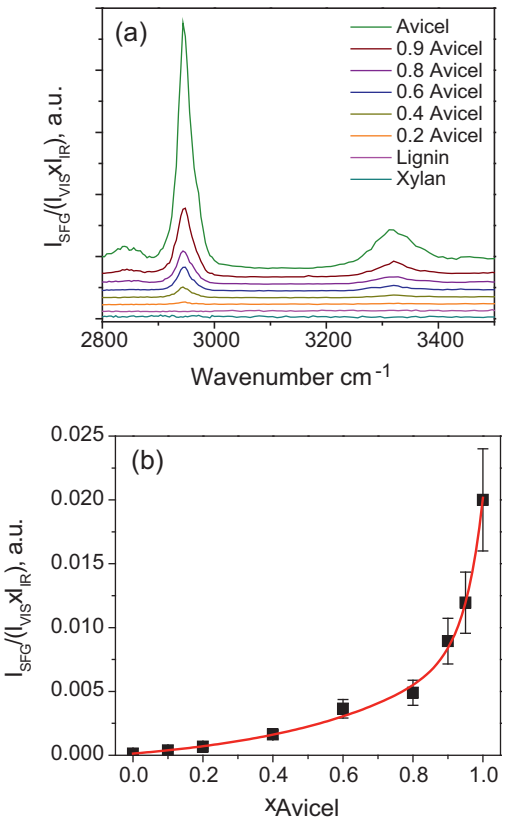

Fig. 1. (a) SFG spectrum from 2800 to 3500 cm^{-1} of physical mixtures containing a mass fraction of Avicel cellulose with the remaining portion a 1:1 mixture of lignin and xylan powders. For display purposes, the SFG intensity values are offset. (b) Plot of SFG intensity of the CH_2 asymmetric stretching vibration peak intensity at 2945 cm^{-1} as a function of mass fraction of cellulose in physical mixtures. The error bars were calculated from measurements with 3 samples and at least 3 locations per sample. The curve fit line is a guide to the nonlinear relationship.

they do not meet the requirement of non-centrosymmetry. For the same reason, H_2O absorbed in the sample is not detected in SFG.

Fig. 1b shows the intensity of the CH_2 asymmetric vibration peak at 2945 cm^{-1} as a function of Avicel mass fraction measured with the model biomass samples. It was found that the SFG intensity varies monotonically but nonlinearly with the amount of crystalline cellulose in the samples. The nonlinearly can origin from several factors. First, the SFG intensity is proportional to the square of the number density of vibration modes that are arranged non-centrosymmetrically in the optical probe volume ($I(\omega_{SFG}) \propto |\chi^{(2)}_{eff}|^2 \propto N^2$; Eqs. (1) and (2)). Although the non-crystalline components in the sample do not generate SFG signals (as demonstrated with xylan and lignin spectra in Fig. 1a), non-cellulosic components can absorb the IR beam needed to generate SFG signal from the crystalline cellulose. Thus, the increases of the non-cellulosic fraction in the sample can result in the decrease of the net intensity of the IR beam absorbed by cellulose ($I(\omega_{IR})$ in Eq. (1)). In addition, lignin can absorb photons in the wavelength region of the SFG signal (460 nm = 532 nm + 2945 cm^{-1}), which can lower SFG photon emission yield from the sample ($I(\omega_{SFG})$ in Eq. (1)) (Austin & Ballaré, 2010; Luo, Zhan, Chai, Fu & Liu, 2009).

Since the SFG intensity varies monotonically with the crystalline cellulose and non-cellulosic components do not produce any SFG signal, it could be possible to construct a calibration curve for estimation of the crystalline cellulose fraction from the measured SFG peak intensity. This will be addressed further in Section 3.2.

3.1.2. XRD analysis

XRD spectra of the same model biomass samples are shown in Fig. 2. Avicel has a main peak at $2\theta = 22.9^\circ$ and the small peaks at 14.9°, 16.7°, and 34.5°. Amorphous xylan and lignin do not display any diffraction peaks but diffuse scattering halos in the 2θ range from ~12° to ~27°, which overlap with the crystalline diffraction peak positions. As the Avicel mass fraction decreases in the model biomass sample, the intensities of the crystalline cellulose diffraction peaks decrease and the broad background increases.

In order to determine the sample crystallinity from the XRD diffractorgram of lignocellulose biomass, the contribution from the amorphous background must be corrected appropriately (Driemeier & Calligaris, 2011; Langan et al., 2005; Park et al., 2010; Wada et al., 2004). The XRD data collected with a powder diffractometer can be analyzed with three different methods: peak height method (square), peak deconvolution method (diamond), and amorphous subtraction method (triangle). Fig. 2b shows the calculation results of the data shown in Fig. 2a. The peak height method, which is the most widely used in the literature, predicts the highest sample crystallinity for each mixture. If the sample crystallinity calculated from the XRD peak intensity is 'true' crystallinity, then the plot of the calculated value against the mass fraction of Avicel should be a straight line in the diagonal direction; but, it is clear that the calculated percentage of crystalline cellulose in the sample does not vary linearly with the actual amount of Avicel. The calculated sample crystallinity decreases only by 22% (from 89% to 67%), while the actual Avicel mass fraction is decreased by 60% (from 100% to 40%). The calculated sample crystallinity is 46% at an Avicel mass fraction of 20%, which is more than 200% error. One of the reasons for the overestimation for the peak height method might be the exclusion of area and width information from diffraction analysis.

An alternative is the peak deconvolution method which utilizes the full spectrum of information. As shown in Fig. 2b, this method gives a somewhat linear correlation with the amount of Avicel. An important assumption for this analysis is that peak broadening is mainly caused by the increased amorphous content in sample. However, there are other intrinsic factors, e.g. crystallite size, which influence peak broadening and intensity in addition to amorphous content.

Another method is the amorphous subtraction method which uses an amorphous standard to subtract the amorphous portion from the diffracted profiles (Thygesen et al., 2005). A challenge is to choose proper amorphous standards that are similar to the amorphous component in the sample. Various materials have been used as amorphous standards such as ball-milled cellulose, regenerated cellulose, and xylan or lignin powder (Park et al., 2010). In this study, the diffuse scattering data was obtained from the xylan and lignin mixture (1:1) as the amorphous standard. Fig. 2b shows that the amorphous subtraction method gives the best linearity. However, which method is more accurate remains an open question; a more advanced calculation method is needed (Driemeier & Calligaris, 2011).

3.1.3. FT-Raman analysis

Fig. 3 displays the Raman spectra of cellulose, xylan, and lignin alongside their physical mixtures. The peak position and relative intensity were consistent with previous reports (Agarwal & Ralph, 1997; Kačuráková et al., 1999). For xylan and cellulose, the peak at 2895 cm^{-1} is the C—H stretch. The peaks at 1382 cm^{-1} and 1405 cm^{-1} are combinations of CCH or OCH, and COH bending modes. The 1471 cm^{-1} is attributed to the CH_2 bending mode. Strong bands at 1097 cm^{-1} and 1120 cm^{-1} are assigned to combinations of stretching of CO or CC ring, COC glycosidic linkages. In the fingerprint region in 300~900 cm^{-1}, several complex modes exist that are highly delocalized over the entire molecule (Agarwal

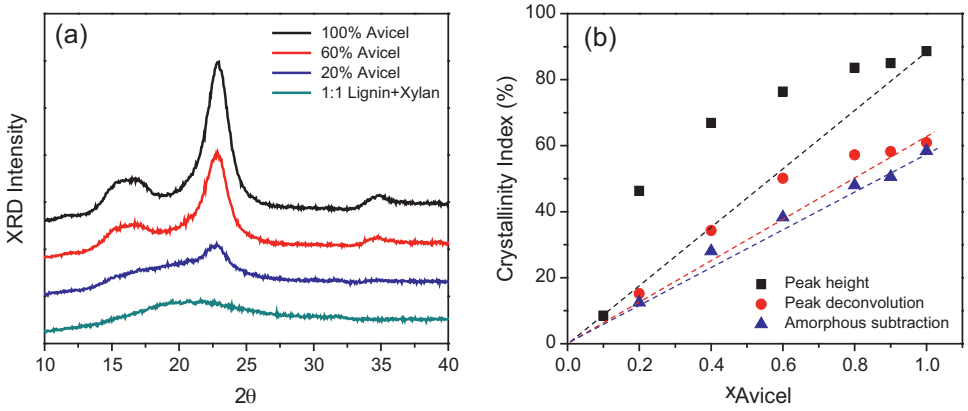

Fig. 2. (a) XRD spectra of model biomass samples; 100% Avicel cellulose, 60% cellulose, 20% cellulose, and 1:1 mixture of xylan and lignin. (b) Sample crystallinity indices calculated from different analysis methods versus actual mass fraction of Avicel cellulose in each model biomass. The dotted lines are a guide to a linear dependence of the calculated crystallinity on the cellulose (Avicel) fraction in the sample.

& Ralph, 1997; Wiley & Atalla, 1987). The Raman spectra of cellulose and xylan have many common peaks. This is because local functional groups are similar in the monomeric carbohydrate units; the only differences are their connections and repetitions in the polymer structure.

Commercially available lignin used in this study gives broad featureless Raman spectra with a few peaks characteristic to phenolic groups of lignin at 1598 cm^{-1} and 1629 cm^{-1}. Notice a broad background increasing at lower wavenumbers due to inelastic scattering from chromophores such as phenolic groups, or other color producing molecules in wood tissues (Kačuráková et al., 1999). The broad absorption and fluorescence behavior of lignin interferes with Raman analysis of cellulose crystallinity in lignocellulosic biomass (Agarwal, 2006; Agarwal & Ralph, 1997). Also, the strong light absorption by lignin can cause sample burning. During data acquisition in this work, the 1064 nm laser beam had to be defocused and lowered in power to prevent the samples from burning. Unfortunately, this lowers the signal-to-noise ratio of the data.

As the lignin and hemicellulose fractions are increased in the physical mixtures, strong cellulose and xylan bands at 2895 cm^{-1}, 1121 cm^{-1} and 1096 cm^{-1} from cellulose and xylan decrease drastically. When the cellulose content is decreased to 60% (lignin content = 20%), the cellulose and xylan peaks become insignificant in a broad featureless background. These can influence the calculation of the sample crystallinity from FT-Raman data. Previously, the intensity ratio of 380 cm^{-1} (based line corrected at 358 cm^{-1}) versus 1096 cm^{-1} (internal reference; baseline corrected at 944 cm^{-1}) and the intensity ratio of the 1481 cm^{-1} crystalline peak versus the 1462 cm^{-1} amorphous peak were demonstrated to be useful to estimate the cellulose crystallinity, i.e. the fraction of crystalline cellulose in pure cellulose samples, which was calculated from XRD (Agarwal et al., 2010; Schenzel et al., 2005). However, due to hemicellulose bands near these features (for example, xylan has a weak peak at 376 cm^{-1} and a strong peak at 1467 cm^{-1}) and high background of the lignin used in this experiment below 2000 cm^{-1}, the accurate measurement of their peak area becomes challenging for complex samples.

3.1.4. FT-IR analysis

Fig. 4 shows the FT-IR spectra from pure and physical mixture samples. The CH stretch region of the FT-IR spectrum (2800–3000 cm^{-1}) is rarely analyzed in detail, because all cellulose, hemicellulose, lignin have similar peak shapes near 2902 cm^{-1} with only minor differences in peak shoulders (Cael et al., 1975; Schwanninger, Rodrigues, Pereira & Hinterstoisser, 2004). More broad features in the OH stretching vibration region

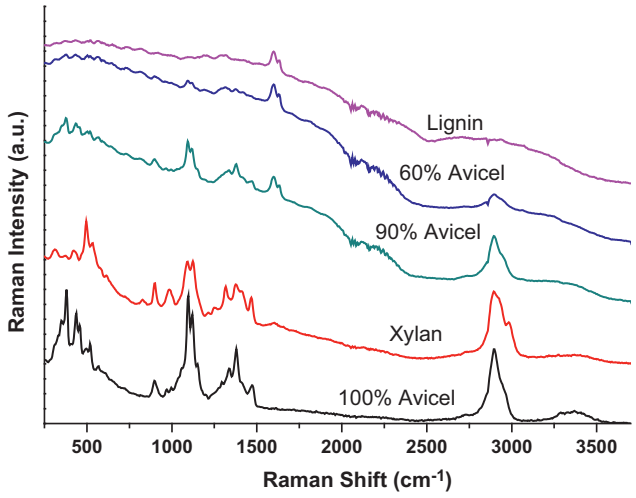

Fig. 3. FT-Raman spectra from 250 to 3750 cm^{-1} of 100% Avicel cellulose, xylan, 90% cellulose, 60% cellulose, and lignin.

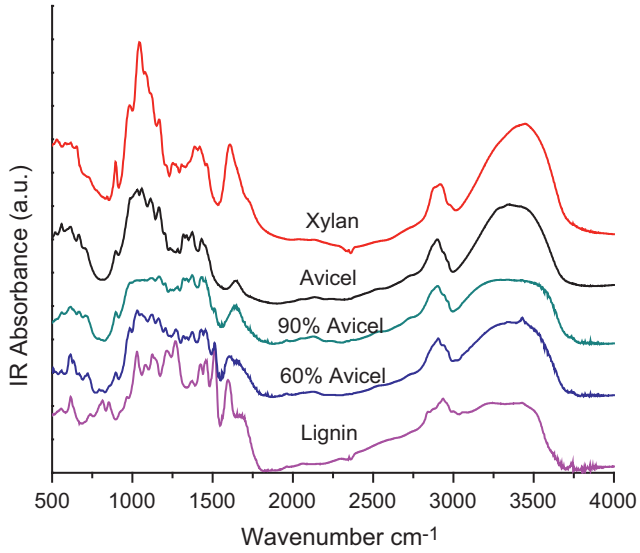

Fig. 4. FT-IR spectra from 500 to 4000 cm^{-1} of pure samples: Avicel cellulose, xylan and lignin, alongside physical mixtures of 90% and 60% cellulose. Each spectrum was normalized at 2907 cm^{-1}.

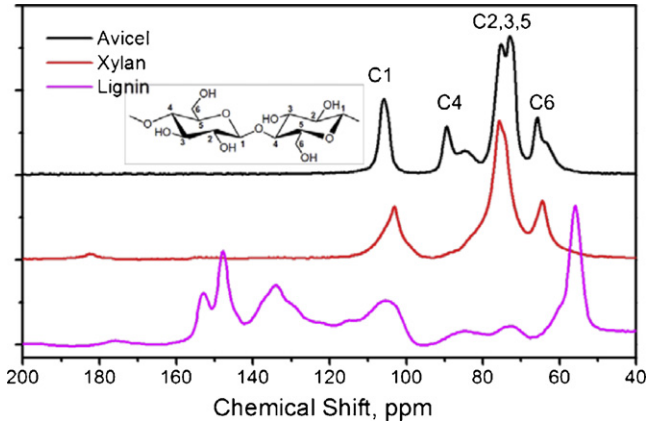

Fig. 5. Solid-state ^{13}C NMR spectrum of Avicel cellulose, xylan, and lignin.

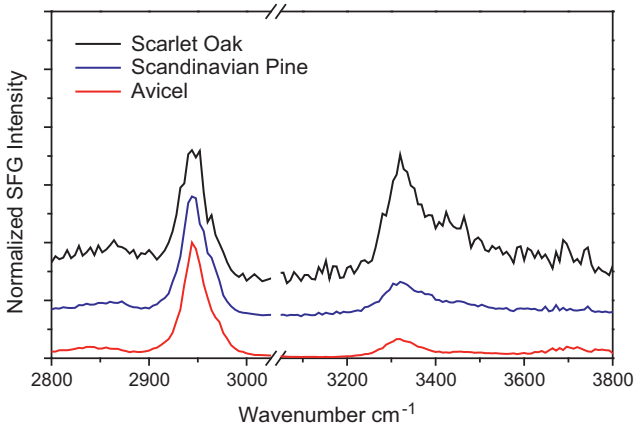

Fig. 6. Normalized SFG spectrum from 2700 to 3800 cm^{-1} of Scarlet oak, Scandinavian pine, and Avicel cellulose. SFG intensity of all samples is normalized at 2945 cm^{-1} and offset for display purposes.

(3000–3700 cm^{-1}) is the consequence of varying degree of hydrogen bonding interactions among hydroxyl groups in the cellulose crystals as well as in hemicellulose and lignin. In addition, there are significant contributions from water absorbed in the amorphous region of the sample (Cael et al., 1975; Frilette, Hanle & Mark, 1948). Due to these reasons, it is practically impossible to distinguish or quantify cellulose, hemicellulose, and lignin in the CH and OH stretch vibration region of FT-IR spectra.

Sharp peaks in the finger print region (500–1600 cm^{-1}) could be used for calculation of cellulose crystallinity. For pure cellulose samples, the intensity ratios of peaks of 1430 cm^{-1} vs. 894 cm^{-1}, 1278 cm^{-1} vs. 1263 cm^{-1}, and 1372 cm^{-1} vs. 894 cm^{-1} have been shown to correlate with the peak height method in XRD (Oh et al., 2005; Schwanninger et al., 2004). However, using these analysis methods becomes extremely difficult in complex lignocellulosic samples because of the proximity of several lignin and hemicellulose bands. In Fig. 4, xylan has peaks at 1428 cm^{-1}, 894 cm^{-1} and lignin has peaks at 1429 cm^{-1}, 1263 cm^{-1}; all of these peaks overlap with crystalline cellulose. In contrast, the lignin quantification can be done relatively easily using the aromatic skeletal vibration peak at 1510 cm^{-1}, because xylan and cellulose do not have a peak at this position.

3.1.5. NMR analysis

Solid-state ^{13}C NMR has been used to evaluate the crystallinity index of cellulose samples. In the NMR spectra in Fig. 5, the peak at 89 ppm is assigned to the C4 carbon in crystalline cellulose structures and the peak at 84 ppm is assigned to the C4 carbon of disordered cellulose (Atalla, 1999). Crystallinity index is then calculated by dividing the area of the crystalline peak by the total area assigned to the C4 peaks. However, analyzing cellulose crystallinity in lignocellulosic biomass is complicated due to the signal overlaps from non-cellulosic components such as hemicellulose and lignin. As shown in Fig. 5, xylan spectrum has a broad and continuous tail in the C4 peak position of cellulose. Aliphatic carbons in lignin also show some intensity in the range of 65–95 ppm. Deconvolution of these signals from non-cellulosic components is possible using complicated cross-polarization pulse sequences. However, the quantitative analysis of cross-polarized NMR data is difficult since the degree of coupling of proton relaxation with neighboring carbons varies depending on structures.

3.2. Characterization of lignocellulosic biomass

To evaluate the potential of SFG to quantify crystalline cellulose in lignocellulosic biomass or 'sample crystallinity', the SFG analysis of wood chips from Scandinavian pine and Scarlet oak was performed. The SFG spectra of these wood samples shown in Fig. 6 look similar to that of Avicel, indicating that non-cellulosic components in wood are not detected in SFG spectra. As mentioned earlier, xylan and lignin do not meet the non-centrosymmetry requirement of the SFG process and thus, they do not give any SFG signal. Only certain vibration modes in crystalline cellulose meet this requirement and produce SFG signals (see Section 3.1.1).

Upon closer inspection, some minor differences can be observed. For example, the shape and intensity of the OH stretching vibration peak are somewhat different for each species. It is speculated that these variations in OH stretching vibrations might originate from interactions between cellulose and hemicellulose components in the secondary cell walls of these wood samples (Fry, 1986; Hayashi, 1989; Levy, York & Stuike-Prill, Meyer, Staehelin, 1991; Pauly, Albersheim, Darvill & York, 1999). Further detailed analysis is necessary to understand the interaction between cell wall components, but it is beyond the scope of this paper.

In this study, an attempt was made to evaluate the feasibility of estimating the amount of crystalline cellulose in wood samples. By applying the calibration curve made with Avicel (Fig. 1b) to the intensity of the CH_2 SFG peak of cellulose at 2945 cm^{-1}, the

Table 1
Sample crystallinity and sugar analysis for Scandinavian pine and Scarlet oak.

	Crystalline cellulose fraction (%) in sample					Sugar analysis, %				
	SFG[a]	Raman[b]	XRD[c]	XRD[d]	XRD[e]	Glucan	Other carbohydrates	Lignin	Extractives	Mass balance
Scandinavian pine	43	41	81	54	40	45	25	27	1.9	99
Scarlet oak	33	49	78	43	29	37	31	25	3.2	96

[a] Avicel-equivalent cellulose content calculated from g the calibration curve shown in (b).
[b] Calculated from Fig. 7 using the univariate method (Agarwal et al., 2010).
[c] Calculated from Fig. 8 using the XRD peak height method (Park et al., 2010).
[d] Calculated from Fig. 8 using the XRD peak deconvolution method (Park et al., 2010).
[e] Calculated from Fig. 8 using the XRD amorphous subtraction method (Park et al., 2010).

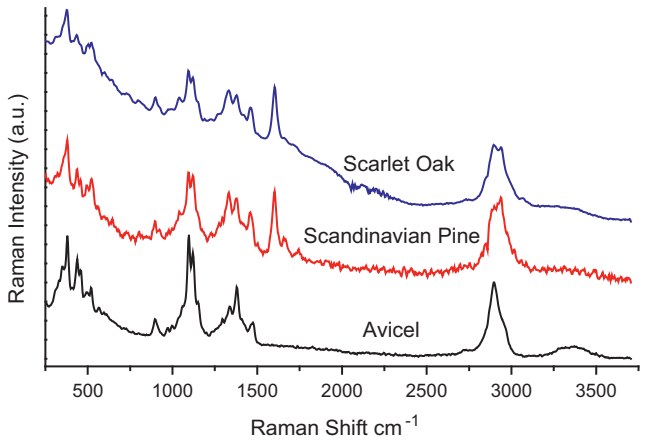

Fig. 7. FT-Raman spectra from 250 to 3750 cm^{-1} of Avicel, and raw wood chip samples of Scarlet oak and Scandinavian pine. Raman intensities of all samples are normalized at 2898 cm^{-1}, and offset for display purposes.

Avicel-equivalent cellulose content was estimated in Table 1. For the pine and oak samples, SFG value at 2945 cm^{-1} were 0.0018 and 0.0012, which correspond to 0.44 and 0.33 in Fig. 1b, respectively. For the procedural purpose, it is assumed in this study that Avicel is highly crystalline cellulose and thus, sample crystallinity can be represented by Avicel-equivalent cellulose content. However, it should be noted that Avicel cellulose is not 100% crystalline and it was estimated about 80% crystalline (Park et al., 2010). The 'Avicel-equivalent' values for Scandinavian pine and Scarlet oak estimated by SFG intensities are compared with the total cellulose contents determined by sugar analysis in Table 1. These values were found close to the amount of glucan measured by sugar analysis. It should be noted that there are several uncertainties such as the suitability of Avicel to represent cellulose in biological systems, chemical interactions between cell-wall components which are lacking in the physical mixtures, and light scattering from grains. In addition, the average size of cellulose crystals might also influence the SFG intensity. Unless all these factors are taken into account, the accuracy of the quantitative SFG analysis of crystalline cellulose in real biomass would be limited.

Table 1 also compares the sample crystallinity of wood samples estimated from FT-Raman and XRD data in Figs. 7 and 8. The lignin backgrounds of these samples in Fig. 7 are much lower than those of commercial lignin shown in Fig. 3. Especially, Scandinavian pine has much lower fluorescence background from lignin compared to Scarlet oak. The fluorescence background from lignin varies with the wood type (Agarwal et al., 2010; Kačuráková et al., 1999). It might be noteworthy that the darker samples tend to give a higher fluorescence background in Raman analysis. Using the univariate method described in elsewhere (Agarwal et al., 2010), the sample crystallinity was estimated to be ~41% for Scandinavian pine and 49% for Scarlet oak, Table 1.

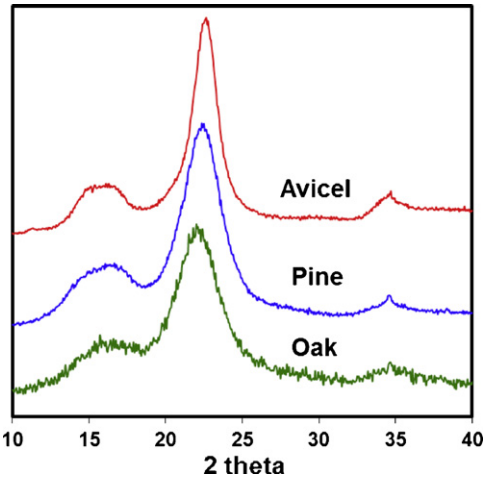

Fig. 8. XRD spectra of Avicel, and raw wood chip samples of Scandinavian pine and Scarlet oak. XRD intensities of all samples are normalized for display purpose.

The sample crystallinity calculation from the XRD results was carried out with the three methods discussed in Fig. 2. It showed reasonable values when the peak amorphous subtraction method was applied, but abnormally high value was estimated with the peak height method. These results affirm that the peak height method, most widely used due to its simplicity, is not appropriate for crystallinity calculation for lignocellulosic biomass samples.

4. Conclusion

The variation of SFG signal with the amount of cellulose in biomass samples was studied using model samples with known concentrations of commercial cellulose, xylan, and lignin. It was found that the SFG intensity is monotonically but nonlinearly with the amount of crystalline cellulose in the samples. This nonlinearity is considered due to several factors such as light scattering and absorption by xylan and lignin as well as the second order dependence of the SFG intensity on the ordered structure. SFG is found highly sensitive over a wide range of crystallinity. In addition, it was attempted to estimate the amount of crystalline cellulose in wood samples based on the calibration curve developed from the model biomass study. The intrinsic selectivity of SFG to crystalline cellulose and insensitivity to amorphous components in the sample resolve some of the difficulties that other conventional analysis methods such as XRD, FT-Raman, FT-IR and NMR have to deal with. Therefore, SFG spectroscopy has great potential as a complementary and sensitive tool to assess the relative amount of crystalline cellulose in lignocellulosic biomass.

Acknowledgments

This work was supported by The Center for Lignocellulose Structure and Formation, an Energy Frontier Research Center funded by the U.S. Department of Energy, Office of Science, and Office of Basic Energy Sciences under Award Number DE-SC0001090. The SFG system was purchased through the support from the Penn State Center for Optical Technologies. We acknowledge Dr. S. Denev and Prof. V. Gopalan for help with SFG system operations and maintenance. The XRD and NMR work was supported by National Research Foundation of Korea under Award Number 2011-0025029.

References

Agarwal, U. P. (2006). Raman imaging to investigate ultrastructure and composition of plant cell walls: Distribution of lignin and cellulose in black spruce wood (*Picea mariana*). *Planta*, *224*(5), 1141–1153.

Agarwal, U. P., & Ralph, S. A. (1997). FT-Raman spectroscopy of wood identifying contributions of lignin and carbohydrate polymers in the spectrum of black spruce (*Picea mariana*). *Applied Spectroscopy*, *51*(11), 1648–1655.

Agarwal, U. P., Reiner, R. S., & Ralph, S. A. (2010). Cellulose I crystallinity determination using FT-Raman spectroscopy: Univariate and multivariate methods. *Cellulose*, *17*(4), 721–733.

Amim, J., Kosaka, P. M., Petri, D. F. S., Maia, F. C. B., & Miranda, P. B. (2009). Stability and interface properties of thin cellulose ester films adsorbed from aceton and ethyl acetate solutions. *Journal of Colloid and Interface Science*, *332*, 477–483.

Atalla, R. H. (1999). Individual structures of native celluloses. In *10th Annual symposium on wood and pulping chemistry: Main symposium* (pp. 608–614). Tabor Press.

Austin, A. T., & Ballaré, C. L. (2010). Dual role of lignin in plant litter decomposition in terrestrial ecosystems. *PNAS*, *107*(10), 4618–4622.

Barnette, A. L., Bradley, L. C., Veres, B. D., Schreiner, E. P., Park, Y. B., Park, J., Park, S., & Kim, S. H. (2011). Selective detection of crystalline cellulose in plant cell walls with sum-frequency-generation (SFG) vibration spectroscopy. *Biomacromolecules*, *12*(7), 2434–2439.

Cael, J. J., Gardner, K. H., Koenig, J. L., & Blackwell, J. (1975). Infrared and Raman spectroscopy of carbohydrates Paper V: Normal coordinate analysis of cellulose I. *Journal of Chemical Physics*, *62*(3), 1145–1153.

Driemeier, C., & Calligaris, G. A. (2011). Theoretical and experimental developments for accurate determination of crystallinity of cellulose I materials. *Journal of Applied Crystallography*, *44*(1), 184–192.

Frilette, V. J., Hanle, J., & Mark, H. (1948). Rate of exchange of cellulose with heavy water. *Journal of the American Chemical Society*, *70*(3), 1107–1113.

Fry, S. C. (1986). Cross-linking of matrix polymers in the growing cell walls of angiosperms. *Annual Review of Plant Physiology*, *37*, 165–186.

Hall, M., Bansal, P., Lee, J. H., Realff, M. J., & Bommarius, A. S. (2010). Cellulose crystallinity - a key predictor of the enzymatic hydrolysis rate. *FEBS Journal*, *277*(6), 1571–1582.

Hatakeyama, T., & Hatakeyama, H. (1982). Temperature depedence of X-ray diffractograms of amorphous lignins and polystyrenes. *Polymer*, *23*(3), 475–477.

Hayashi, T. (1989). Xyloglucans in the primary cell wall. *Annual Review of Plant Physiology and Plant Molecular Biology*, *40*, 139–168.

Held, H., Lvovsky, A. I., Wei, X., & Shen, Y. R. (2002). Bulk contribution from isotropic media in surface sum-frequency generation. *Physical Review B*, *66*(20), 205110.

Hindeleh, A. M., & Johnson, D. J. (1972). Crystallinity and crystallite size measurement in cellulose fibres: 1. Ramie and fortisan. *Polymer*, *13*(9), 423–430.

Hindeleh, A. M., & Johnson, D. J. (1974). Crystallinity and crystallite size measurement in cellulose fibres: 2. Viscose rayons. *Polymer*, *15*(11), 697–705.

Isogai, A. (Ed.). (1994). *Allomorphs of cellulose and other polysaccharides*. Munich: Hanser.

Isogai, A., Usuda, M., Kato, T., Uryu, T., & Atalla, R. H. (1989). Solid-state CP/MAS 13C NMR Study of cellulose polymorphs. *Macromolecules*, 3168–3172.

Jarvis, M. (2003). Cellulose stacks up. *Nature*, *426*(6967), 611–612.

Kačuráková, M., Weller, N., Ebringerová, A., Hromádková, Z., Wilson, R. H., & Belton, P. S. (1999). Characterisation of xylan-type polysaccharides and associated cell wall components by FT-IR and FT-Raman spectroscopies. *Food Hydrocolloids*, *13*, 35–41.

Katoaka, Y., & Kondo, T. (1998). FTIR microscopic analysis of changing cellulose crystalline structure during wood cell wall formation. *Macromolecules*, *31*(3), 760–764.

Kim, J., Yun, S., & Ounaies, Z. (2006). Discovery of cellulose as a smart material. *Macromolecules*, *39*(12), 4202–4206.

Kondo, T. (1997). The assignment of IR adsorption bands due to free hydroxyl groups in cellulose. *Cellulose*, *4*(4), 281–292.

Kondo, T., & Sawatari, C. (1996). A Fourier transform infra-red spectroscopic analysis of the character of hydrogen bonds in amorphous cellulose. *Polymer*, *37*(3), 393–399.

Kono, H., Erata, T., & Takai, M. (2002). CP/MAS 13C NMR study of cellulose and cellulose derivatives. 2. Complete assignment of the 13C resonance for the ring carbons of cellulose triacetate polymorphs. *Journal of the American Chemical Society*, *124*(25), 7512–7518.

Kono, H., Yunoki, S., Shikano, T., Fujiwara, M., Erata, T., & Takai, M. (2002). CP/MAS 13C NMR study of cellulose and cellulose derivatives. 1. Complete assignment of the CP/MAS 13C NMR spectrum of the native cellulose. *Journal of the American Chemical Society*, *124*(25), 7506–7511.

Kovalenko, V. I. (2010). Crystalline cellulose: Structure and hydrogen bonds. *Russian Chemical Reviews*, *79*(3), 231–241.

Lambert, A. G., Davies, P. B., & Neivandt, D. J. (2005). Implementing the theory of sum frequency generation vibrational spectroscopy: A tutorial review. *Applied Spectroscopy Reviews*, *40*(2), 103–145.

Langan, P., Sukumar, N., Nishiyama, Y., & Chanzy, H. (2005). Synchrotron X-ray structures of cellulose Iβ and regenerated cellulose II at ambient temperature and 100 K. *Cellulose*, *12*(6), 551–562.

Levy, S., York, W. S., Stuike-Prill, R., Meyer, B., & Staehelin, A. (1991). Simulations of the static and dynamic molecular conformations of xyloglucan. The role of the fucosylated sidechain in surface-specific sidechain folding. *Plant Journal*, *1*(2), 195–215.

Luo, X., Zhan, H., Chai, X.-S., Fu, S., & Liu, J. (2009). A novel method for determination of aromatic aldehyde monomers in lignin degradation liquor. *Industrial and Engineering Chemistry Research*, *48*(5), 2713–2716.

Marrinan, H. J., & Mann, J. (1954). A study by infra-red spectroscopy of hydrogen bonding in cellulose. *Jornal of Applied Chemistry*, *4*(4), 204–211.

Meier, R. J. (2005). On art and science in curve-fitting vibrational spectra. *Vibrational Spectroscopy*, *39*(2), 266–269.

Meyer, K. H., & Misch, L. (1937). Positions des atomes dans le nouveau modele spatial de la cellulose. *Helvetica Chimica Acta*, *20*(1), 232–244.

Miranda, P. B., & Shen, Y. R. (1999). Liquid interfaces: A study by sum-frequency vibrational spectroscopy. *Journal of Physical Chemistry B*, *103*

Oh, S. Y., Yoo, D. I., Shin, Y., Kim, H. C., Kim, H. Y., Chung, Y. S., et al. (2005). Crystalline structure analysis of cellulose treated with sodium hydroxide and carbon dioxide by means of X-ray diffraction and FTIR spectroscopy. *Carbohydrate Research*, *340*(15), 2376–2391.

Park, S., Baker, J. O., Himmel, M. E., Parilla, P. A., & Johnson, D. K. (2010). Cellulose crystallinity index: Measurement technique and their impact on interpreting cellulose data. *Biotechnology for Biofuels*, *3*, 10.

Park, S., Johnson, D. K., Ishizawa, C. I., Parilla, P. A., & Davis, M. F. (2009). Measuring crystallinity index by solid state ^{13}C NMR. *Cellulose*, *16*(4), 641–647.

Pauly, M., Albersheim, P., Darvill, A., & York, W. S. (1999). Molecular domains of the cellulose/xyloglucan network in the cell walls of higher plants. *Plant Journal*, *20*(6), 629–639.

Pérez, S., & Samain, D. (2010). Structure and Engineering of Celluloses. *Advances in Carbohydrate Chemistry and Biochemistry*, *64*, 25–116.

Schenzel, K., Fischer, S., & Brendler, E. (2005). New method for determining the degree of cellulose I crystallinity by means of FT Raman spectroscopy. *Cellulose*, *12*(3), 223–231.

Schindelman, G., Morikami, A., Jung, J., Baskin, T. I., Carpita, N. C., Derbyshire, P., et al. (2001). COBRA encodes putative GPI-anchored protein, which is polarly localized and necessary for oriented cell expansion in Arabidopsis. *Genes and Development*, *15*, 1115–1127.

Schwanninger, M., Rodrigues, J. C., Pereira, H., & Hinterstoisser, B. (2004). Effects of short-time vibratory ball milling on the shape of FT-IR spectra of wood and cellulose. *Vibrational Spectroscopy*, *36*(1), 23–40.

Segal, L., Creely, J. J., Martin, A. E., & Conrad, C. M. (1959). An empirical method for estimating the degree of crystallinity of native cellulose using the X-ray diffractometer. *Textile Research Journal*, *29*(10), 786–794.

Shen, Y. R. (1989). Surface properties probed by second-harmonic and sum-frequency generation. *Nature*, *337*(9), 519–525.

Sluiter, A., Hames, B., Ruiz, R., Scarlata, C., Sluiter, J., Templeton, D., et al. (2008). *Determination of structural carbohydrates and lignin in biomass (vol. standard biomass analytical procedures)*. Golden, CO, USA: National Renewable Energy Laboratory.

Thygesen, A., Oddershede, J., Lilholt, H., Thomsen, A. B., & Ståhl, T. K. (2005). On the determination of crystallinity and cellulose content in plant fibers. *Cellulose*, *12*(6), 563–576.

Vidal, F., & Tadjeddine, A. (2005). Sum-frequency generation spectroscopy of interfaces. *Reports on Progress in Physics*, *68*(5), 1095–1127.

Wada, M., Chanzy, H., Nishiyama, Y., & Langan, P. (2004). Cellulose IIII crystal structure and hydrogen bonding by synchrotron X-ray and neutron fiber diffraction. *Macromolecules*, *37*(23), 8548–8555.

Wada, M., Ike, M., & Tokuyasu, K. (2010). Enzymatic hydrolysis of cellulose I is greatly accelerated via its conversion to the cellulose II hydrate form. *Polymer Degradation and Stability*, *95*(4), 543–548.

Wan, J. Q., wang, Y., & Xiao, Q. (2010). Effects of hemicellulose removal on cellulose fiber structure and recycling characteristics of Eucalyptus pulp. *Bioresource Technology*, *101*(12), 4577–4583.

Whitney, S. E. C., Brigham, J. E., Darke, A. H., Grant Reid, J. S., & Gidley, M. J. (1995). In vitro assembly of cellulose/xyloglucan networks: Ultrastructural and molecular aspects. *Plant Journal*, *8*(4), 491–504.

Wiley, J. H., & Atalla, R. H. (1987). Band assignments in the Raman spectra of celluloses. *Carbohydrate Research*, *160*(15), 113–129.

Zhang, Y.-H. P., & Lynd, L. R. (2004). Toward an aggregated understanding of enzymatic hydrolysis of cellulose: Noncomplexed cellulase systems. *Biotechnology and Bioengineering*, *88*(7), 797–824.

Zhao, W., & Berg, v. D. A. (2008). Lab on paper. *Lab on a Chip*, *8*, 1988–1991.